Bioactive Constituents, Metabolites, and Functions

RDP3, A Novel Anti-Gout Peptide Derived from Water Extract of Rice.

Naixin Liu, Ying Wang, Lin Zeng, Saige Yin, Yan Hu, Shanshan Li, Yang Fu, Xinping Zhang, Chun Xie, Longjun Shu, Yilin Li, Huiling Sun, Meifeng Yang, Jun Sun, and Xinwang Yang

J. Agric. Food Chem., **Just Accepted Manuscript** • DOI: 10.1021/acs.jafc.0c02535 • Publication Date (Web): 16 Jun 2020

RDP3, A Novel Anti-Gout Peptide Derived from Water Extract of Rice

Naixin Liu[†, ‡], Ying Wang[§, †], Lin Zeng[//], Saige Yin[‡], Yan Hu[‡], Shanshan Li[‡], Yang Fu[‡], Xinping Zhang[‡], Chun Xie[‡], Longjun Shu[§], Yilin Li[‡], Huiling Sun[‡], Meifeng Yang[‡], Jun Sun[‡, *], Xinwang Yang[‡, *]

[‡]Department of Anatomy and Histology & Embryology, Faculty of Basic Medical Science, Kunming Medical University, Kunming, Yunnan, China, 650500.

[§]Key Laboratory of Chemistry in Ethnic Medicine Resource, State Ethnic Affairs Commission & Ministry of Education, School of Ethno-Medicine and Ethno-Pharmacy, Yunnan Minzu University, Kunming, Yunnan, China, 650504.

[//]Public Technical Service Center, Kunming Institute of Zoology, Chinese Academy of Sciences, Kunming, Yunnan, China, 650223.

[†]**These authors contributed equally to this work**

[*]**Corresponding authors:**

Prof. Xinwang Yang, Faculty of Basic Medical Science, Kunming Medical University,1168 West Chunrong Road, Kunming, Yunnan, China, 650500. Email: yangxinwanghp@163.com, telephone: +86 13577174345.

Prof. Jun Sun, Faculty of Basic Medical Science, Kunming Medical University,1168 West Chunrong Road, Kunming, Yunnan, China, 650500. Email: sunjun6661@126.com, telephone: +86 13888438589.

Abstract

Gout and hyperuricemia can seriously affect quality of life; at present, however, existing medicines are unable to meet all clinical needs. In the current study, a novel peptide (i.e., rice-derived-peptide-3 (RDP3), AAAAMAGPK-NH_2, 785.97 Da) in water extract obtained from shelled *Oryza sativa* fruits was identified. Testing revealed that RDP3 (minimum effective concentration 100 μg/kg) showed no both hemolytic and acute toxicity, and reduced uric acid levels in the serum of hyperuricemic mice by inhibiting xanthine oxidase activity and decreasing urate transporter 1 expression. RDP3 also alleviated renal injury in hyperuricemic mice by decreasing NLRP3 inflammasome expression. Furthermore, RDP3 alleviated formalin-induced paw pain and reduced monosodium-urate-crystal-induced paw swelling and inflammatory factors in mice. Thus, this newly identified peptide reduced uric acid levels & renal damage in hyperuricemic mice and showed anti-inflammatory & analgesic activities, indicating the potential of RDP3 as an anti-gout medicine candidate.

Keywords: anti-gout peptide; nutraceutical peptide; hyperuricemia treatment; renal protective peptides; anti-inflammation peptides

Introduction

Gout is a common and complex form of arthritis. It is related to purine metabolism disorders, which cause excessive uric acid production or poor uric acid excretion, with subsequent induction of hyperuricemia (HUA)[1]. Clinically, HUA is diagnosed when the level of serum uric acid is higher than 420 μM in men and 360 μM in women[2]. Continuous HUA can not only lead to an attack of gouty arthritis, but can also cause kidney damage, cardiovascular events, and diabetes[1,3]. In addition, if HUA is not properly treated and controlled, the recurrence, frequency, and degree of gout attack can also increase. Therefore, gout is best treated by controlling HUA[4]. The concentration of uric acid in blood is primarily determined by the absorption and production of purine and by the decomposition and excretion of uric acid[5]. Xanthine oxidase (XOD), a key enzyme for the formation of uric acid, is a major target of inhibitory drugs[5] such as allopurinol and febuxostat[4]. During the process of uric acid metabolism in humans, about 65% of uric acid is filtered through the glomeruli, with 90% then reabsorbed into circulation through urate transporter-related proteins (such as URAT1) and the rest filtered into urine for excretion[5]. Anti-hyperuricemic medicines, such as probenecid and benzbromarone, can significantly enhance the excretion of uric acid by inhibiting URAT1[6]. Currently, treatment of acute gout attack depends on drugs such as nonsteroidal-anti-inflammatory drugs (NSAIDs), colchicine, glucocorticoids, and IL-1β antagonists[4]. However, their clinical use has several limitations. For example, NSAIDs can induce peptic ulcers; allopurinol can produce severe skin rash and allergic reactions; febuxostat can lead to

cardiovascular events; benzbromarone can induce hepatotoxic activity; and probenecid can generate uric acid crystals in the kidney[7-10]. Therefore, the development of new anti-gout drugs remains an important focus.

In recent years, peptide medicines have attracted increasing attention due to their high specificity, high efficiency, limited side effects, and low cost[11-13]. At present, the clinical use of several peptides, such as exenatide and ACEI, are not only more convenient for patients, but also provide considerable economic benefits for society[14, 15]. A large number of other active peptides, such as antibacterial, analgesic, and neuroprotective peptides, have also been identified[16, 17]. To date, however, reports on active peptides that can effectively treat gout and HUA remain scarce[11-13, 18-20]. Therefore, research on peptides for gout and HUA treatment is still in its infancy.

In this study, a short peptide, named rice-derived-peptide-3 (RDP3), obtained from the water extract of shelled *Oryza sativa* fruits from Yunnan, China, was identified. The purpose of this research was to discover an anti-HUA or anti-gout bioactive peptide from *O. sativa* extract that could be used as a potential candidate for the development of anti-gout drugs. We also established a HUA mouse model to explore the mechanism and function of the peptide using various biochemical experiments (i.e., western blotting and ELISA).

Materials & Methods

Sample Purification & Synthesis

Sample Preparation

The shelled *O. sativa* fruits was obtained from Yunnan province and water extract of shelled *O. sativa* fruits was obtained as follows[11]. The rice (shelled *O. sativa* fruits, 1 kg) was first soaked in deionized water (1 L) at 4 °C for 12 h, with the liquid then filtered by filter paper. The resulting solution was centrifuged for 20 min at 4 °C and 12 000 *g*, with the supernatant then collected as the water extract of rice. The obtained liquid was freeze-dried and then stored at −80 °C until analysis.

Purification Procedures

Peptide purification was performed as per our previous report, with some modification[21]. The water extract of rice was purified using a Sephadex G-50 gel filtration column (1.5 × 31 cm, superfine, GE Healthcare, Stockholm, Sweden). The 25 M Tris HCl buffer containing 0.1 M NaCl (pH 7.8) was used for pre-balance and elution at a flow rate of 0.3 ml/min and injection volume of 1 mL. Samples were collected (10 min/tube) with an automatic fractionation collector (BSA-30A, HuXi Company, Shanghai, China), with absorbance then detected at 280 nm (Fig. S1A, same as our previous study[10]). The components represented by the arrow in Fig. S1A were collected, combined, and then injected into a C18 high-performance liquid chromatography (HPLC) column (Hypersil BDS C18, 4.0×300 mm, Elite, China) at an injection volume of 1 mL, with a detection wavelength of 220 nm. Ultrapure water with 0.1% (V/V) trifluoroacetic acid (TFA) was used for pre-balancing and acetonitrile (ACN) with 0.1% (V/V) TFA was eluted at a flow rate of 1 mL/min through a linear gradient (0–40% ACN, 40 min, Fig. S1B, as shown in our previous research[10]). The component

indicated by an arrow in Fig. S1C was collected and a second round of HPLC was performed as above.

Determination of Primary Structure of Peptide

The molecular mass of the sample was detected by mass spectrometry. The sample and α-cyano-4-hydroxycinnamic acid (5 mg/mL, dissolved in 50% ACN, 0.1% TFA) were mixed to a volume, then 1 μL mixture was spotted on a steel plate for crystallization at room temperature. The crystallized sample on the plate was examined via mass spectrometry (Autoflex speed TOF/TOF, Bruker Daltonik GmbH, Leipzig, Germany) for MS and MS/MS analysis in positive charge mode. The ion source voltage for MS analysis were: UIS1: 19KV, UIS2: 16.45KV; The ion source voltage for MS/MS analysis were: UIS1: 6KV, UIS2: 5.15KV. The reflector detector voltage for MS and MS/MS data acquisition were set as 1.942KV and 2.163KV, respectively. FlexAnalysis3.3 and Biotools 3.2 provide by manufacturer were used for MS and MS/MS spectra interpretation. Mass tolerance of MS/MS ions was set as ±0.5 Da. The sample was then dissolved in 25 mM NH_4HCO_3 and reduced using dithiothreitol at 37 °C for 1 h, then blocked by iodoacetamide for 30 min. Finally, the mixture was mixed with α-cyano-4-hydroxycinnic acid and analyzed by tandem mass spectrometry on the same equipment. The RDP3 peptide (AAAAMAGPK-NH2) was synthesized at a purity of >95% by Wuhan Bioyeargene Biotechnology Co., Ltd. (Wuhan, China).

Animal Care

Kunming and nude mice (25 ± 5 g) were obtained from Hunan Slack Jingda

Laboratory Animal Co., Ltd. (Hunan, China). All mice were housed in cages (330 × 205 × 180 mm, five mice per cage) at room temperature (22 ± 2 °C), with free access to food and water. All animal handling was implemented in accordance with the Provisions and General Recommendations of the Chinese Experimental Animals Administration Legislation. All animal care and handling procedures were conducted in accordance with the requirements of the Ethics Committee of Kunming Medical University (KMMU20180012).

Characteristics of RDP3

Hemolytic Activity & Acute Toxicity Assays

Hemolytic activity was examined as per earlier experiments, with some modifications[22]. Firstly, human red blood cells (Kunming Blood Center, Kunming, Yunnan, China) were mixed with saline and centrifuged at 3 000 *g* for 5 min at 4 °C to obtain 100% red blood cells. The saline was used as the solvent. Different doses of RDP3 (500 μL, 100 μg/mL, 500 μg/mL, 1 mg/mL) were gently mixed with the red blood cells (500 μL) and incubated at 37 °C for 30 min. The mixture was then centrifuged at room temperature (22 ± 2 °C) for 4 min at 4 000 *g*. Finally, the supernatant was tested at 540 nm, with 0.1% Triton X-100 used as the positive control to determine the maximum hemolysis rate (n = 5).

Acute toxicity was investigated following previous research[22]. Briefly, different doses of RDP3 (100 μg/kg, 500 μg/kg, 1 mg/kg) and saline (1 mL/kg) were injected into the abdominal cavity of mice. The mortality and general situation of animals in each group were observed and recorded within 24 h (n = 3).

Stability of RDP3

The stability of RDP3 was determined according to previous research, with some modifications[21]. In brief, 100 μL of mouse plasma and 100 μL of RDP3 (10 μg/mL) were mixed, incubated at 37 °C, then tested every 2 h. To terminate the reaction, 219 μl of urea (8 M) and 60 μL of trichloroacetic acid (1 g/mL) were added to the mixture. The supernatant was obtained by centrifuging the mixture at 12 000 *g* for 30 min at 4 °C, which was then collected to determine peptide amount using HPLC.

After the prepared solution (containing RDP3, 10 μg/mL) was repeatedly frozen overnight (at −20 °C) and thawed (at 37 °C), the residual content of the peptide was detected by HPLC. Its stability under different temperatures was also researched. Specifically, RDP3 (10 μg/mL) was incubated at 4 °C, 37 °C, and 60 °C for 20 days, with samples collected every 2 days. After centrifugation at 12 000 *g* for 20 min at 4 °C, the supernatant was collected and tested using HPLC.

RDP3 stability tests were determined by HPLC. In summary, the samples (injection volume of 1 mL) were tested using a C18 HPLC column pre-balanced with ultrapure water containing 0.1% (V/V) TFA and with ACN containing 0.1% (V/V) TFA. Elution was conducted at a flow rate of 1 mL/min (0%–30% ACN, 30 min) and monitored at 220 nm. Peak area (elution time) chromatography was used to determine and quantify RDP3 residue.

Distribution of RDP3 In Vivo After Injection

The fluorescein-isothiocyanate-AAAAMAGPK-NH2 (FITC-RDP3) sample was provided commercially by Wuhan Bioyeargene Biotechnology Co., Ltd. (Wuhan,

China). First, nude mice were anesthetized with pentobarbital sodium (3.5%, 100 μL/10 g) and fixed, followed by abdominal injection of 100 μL of FITC-RDP3 (10 μg/μL). Front and back images of mice were then taken and examined at 0 min and 60 min after the injection using a FluorVivo^{TM}300 (Huanya Technology Co., Ltd., Beijing, China).

Anti-hyperuricemic Activity of RDP3

Establishment of HUA Mice

Animal assays were performed according to previous research[23]. Mice were randomly divided into various groups, namely, control, model, allopurinol (Allo, positive group), benzbromarone (Benz, positive group), and RDP3 groups (100 μg/kg, 500 μg/kg, and 1 mg/kg). From day 1 to 7, the mice in the control group were given 1 mL of saline per day, whereas the other groups were treated by intragastric administration of 300 mg/kg potassium oxonate (POX, Dalian Meilun Biological Technology Co., Ltd., Dalian, Liaoning, China) and 200 mg/kg adenine (Dalian Meilun Biological Technology Co., Ltd., Dalian, Liaoning, China) per day. One hour after POX and adenine treatment, saline was given to mice in the control and model groups, whereas the positive groups were treated by intraperitoneal injection of Allo (10 mg/kg, Dalian Meilun Biological Technology Co., Ltd., Dalian, Liaoning, China) or Benz (8 mg/kg, Dalian Meilun Biological Technology Co., Ltd., Dalian, Liaoning, China) and the RDP3 groups were treated by intraperitoneal injection of different doses of RDP3 (100 μg/kg, 500 μg/kg, and 1 mg/kg). Blood and tissue samples were obtained on day 7 after the last administration of RDP3, Allo, or saline. Briefly, 1 h

after the last administration, the mice were anesthetized with 0.3% pentobarbital sodium and blood was taken from the inner canthus vein, followed by rapid removal of liver and kidney tissues on ice. The whole blood samples were centrifuged at 6 000 *g* for 5 min at room temperature (22 ± 2 °C) to obtain serum. The kidneys and livers of mice were stored at −80 °C, with portions of the kidneys fixed in 4% formaldehyde.

Detection of Uric Acid & Creatinine Levels in HUA Mice

Serum levels of uric acid and creatinine were measured using uric acid and creatinine kits per the manufacturer's operational instructions (Nanjing Jiancheng Bioengineering Institute, Nanjing, Jiangsu, China).

Hematoxylin & Eosin (H&E) Staining

H&E staining was performed according to prior study[11]. Kidneys of mice were fixed in 4% formalin for 24 h to 48 h, then dehydrated using gradient ethanol (75% 12 h, 85% 12 h, 95% and 100% 2 h, respectively). Tissues were then embedded in paraffin and sliced to a thickness of 5 μm, followed by H&E staining and visualization via light microscopy (Zeiss, Germany) at 100× magnification.

Molecular Docking

Molecular docking of RDP3-XOD and RDP3-URAT1 complexes was conducted to explore the mechanism related to the lowering of uric acid by RDP3[24]. Briefly, the X-ray crystal structure of XOD was downloaded from the Protein Data Bank (PDB-ID: 2ckj) (http://www.rcsb.org/pdb). The URAT1 architecture was modeled from scratch using the Robetta server (http://www.robetta.org/). The RDP3 structure was

198 constructed using the PEP-FOLD3 server (http://bioserv.rpbs.univ-paris-
199 diderot.fr/services/PEP-FOLD3/). Vina 1.1.2 was used for molecular docking and the
200 conformation with the best affinity (lowest value) was chosen as the docking
201 conformation. Results were then analyzed using Pymol and DS3.5 software.

202 ***Detection of XOD In Vivo and In Vitro***

203 XOD activity in the serum and liver of HUA mice was measured using specific
204 XOD kits (Nanjing Jiancheng Bioengineering Institute, Nanjing, Jiangsu, China), and
205 the IL-1β level in the serum of mice was tested using mouse IL-1β ELISA kits
206 (Shenzhen NeoBioscience Biotechnology Co., Ltd., Shenzhen, China) following the
207 instructions provided by the manufacturer.

208 XOD inhibition *in vitro* was carried out following previous research, with some
209 modifications[12]. The 50 mM Tris-HCl (pH = 8) buffer was prepared as the solvent.
210 The 2 mM xanthine (Dalian Meilun Biological Technology Co., Ltd., Dalian, Liaoning,
211 China) and 0.52 mM XOD (Dalian Meilun Biological Technology Co., Ltd., Dalian,
212 Liaoning, China) solutions were respectively dissolved in the above solvent. The
213 xanthine solution (128 μL), XOD solution (16 μL), RDP3 solution (32 μL, 100 μg/kg,
214 500 μg/kg, and 1 mg/kg), and Tris-HCl buffer (928 μL) were mixed and incubated at
215 37 °C for 15 min. Afterwards, 48 μL of 1 M HCl was used to terminate the reaction,
216 with absorbance then detected at 292 nm. Allo (10 mg/mL) and Tris-HCl buffer were
217 used as the positive and negative controls, respectively. Inhibitory activity was
218 calculated as follows:

219 $$\text{XOD inhibition rate } (\%) = 100\% * \frac{\text{Negative control} - \text{Sample}}{\text{Negative control}}$$

220 ***Detection of IL-1β Levels in Serum of HUA Mice***

221 The IL-1β levels in the serum of mice were tested using mouse IL-1β ELISA kits
222 (Shenzhen NeoBioscience Biotechnology Co., Ltd., Shenzhen, China) following the
223 instructions provided by the manufacturer.

224 ***Western Blotting***

225 Western blot analysis was performed following previous study[25]. Protein from
226 kidney samples was extracted using 20 mg/150 μL RIPA and PMSF (Dalian Meilun
227 Biotechnology Co., Ltd., Dalian, Liaoning, China) at a ratio of 100:1 following the
228 manufacturer-provided instructions. A BCA protein analysis kit (Dalian Meilun
229 Biotechnology Co., Ltd., Dalian, Liaoning, China) was used to detect protein content.
230 Sulfate polyacrylamide gel electrophoresis (SDS-PAGE) was used to detect the
231 URAT1 and NLRP3 inflammasome contents in the kidneys. Protein was separated
232 by 10% SDS-PAGE and transferred to polyvinylidene fluoride (PVDF) membranes.
233 After sealing with 5% skimmed milk for 2 h, the membranes were incubated with
234 primary antibody (GAPDH, URAT1, NLRP3, ASC, Caspase 1, Proteintech, Shanghai
235 Sixin Biotechnology Co., Ltd., Shanghai, China) overnight at 4 °C, and then with
236 secondary antibody (anti-rabbit, Proteintech, Shanghai Sixin Biotechnology Co., Ltd.,
237 Shanghai, China) for 1 h at room temperature (22 ± 2 °C). Membranes were finally
238 analyzed and quantified by Image J software.

239 **Anti-gout Activity of RDP3**

240 ***Anti-inflammatory & Analgesic Activities of RDP3***

241 As per previous research[26], mice were pretreated with saline, diclofenac sodium

(DS, 12 mg/kg), or different concentrations of RDP3 (100 μg/kg, 500 μg/kg, and 1 mg/kg) via intraperitoneal injection. Saline was used as a negative control and DS was used as a positive control. After 30 min, mice were injected with 20 μl of 0.92% formalin under the skin of the right paw, and then placed in cages (20 × 40 × 15 cm) individually. Time spent paw licking by each mouse was recorded (0–5 min and 15–30 min after injection).

Monosodium urate (MSU) crystals were prepared according to previous research[27]. Mice were divided into five groups (n = 6): i.e., 1) Model group, treated with saline; 2) Positive group, treated with 12 mg/kg DS; 3) RDP3 groups, treated with different concentrations RDP3 (100 μg/kg, 500 μg/kg, and 1 mg/kg, respectively). The mice received an intraperitoneal injection once daily. On day 3, 30 min after injection, MSU crystals (20 mg/mL) were injected into the left paw of mice. Subsequent inflammation was quantified by measuring paw thickness with a digital thickness gauge (Hong Kong Dinghao Measuring Tool Co., Ltd., Hongkong, China) on days 1, 2, and 3 after MSU crystal injection. The percentage of edema was calculated as follows:

$$\text{Result} = 100\% \times \left(\frac{b - a}{a}\right)$$

where “a” is paw thickness before MSU crystal injection and “b” is paw thickness after MSU crystal injection.

Paw Inflammation Cytokine Assays & H&E Staining

The levels of IL-1β and TNF-α in mouse feet were tested using specific mouse IL-1β and TNF-α ELISA kits (Shenzhen NeoBioscience Biotechnology Co., Ltd,

Shenzhen, China). All operations were carried out according to the instructions provided by the manufacturer. H&E staining was performed following the procedures used for kidneys, with treated sections visualized via light microscopy (Zeiss, Germany) at 100× magnification.

Results & Discussion

Separation and Identification of RDP3 From Shelled *O. sativa* Fruits

Water extract from shelled *O. sativa* fruits was separated using a Sephadex G-50 gel filtration column. The sample indicated by an arrow in Fig. S1A (Fig. 1A in previous research[11]) was collected and further separated and purified by RP-HPLC, as shown in Fig. S1B. The sample indicated by an arrow in Fig. S1B (corresponding to Fig. 1B in previous research[11], but with different separation peaks) was again purified using HPLC to obtain the sample with an elution time of 16.8 min (as shown in Fig. S1C). The final sample was analyzed by mass spectrometry.

As shown in Fig. 1A, a peptide triplet with a single isotope M/Z of 786.432-808.421-824.400 was observed in the sample. Tandem mass spectrometry was further used to elucidate the sequence of the peptide triplet. The MS/MS spectra showed that the mother ions with M/Z of 786.432, 808.421, and 824.400 represented the [M+H]+, [M+Na]+, and [M+k]+ types, respectively (Fig. 1B), confirming that the sequence of the sample was “AAAAMAGPK-NH2”.

RDP3 Showed No Hemolytic Activity or Acute Toxicity

To evaluate the safety of RDP3, hemolytic activity and acute toxicity were tested. As shown in Tables S1 and S2, RDP3 showed no such activity or toxicity.

Stability of RDP3 & Distribution in Liver & Kidney After Injection

To explore the characteristics of RDP3, its stability under different conditions was measured. As shown in Fig. 2A, after repeated freezing and thawing (12 times), the non-degraded content of RDP3 in the prepared test solution was about 80%; after 20 times, however, RDP3 content was completely degraded. After 20 days, the content of RDP3 at 4 °C and 37 °C was stable, with residual content of 90% and 80%, respectively. After 20 days at 60 °C, the residual RDP3 content was about 20%. The stability of RDP3 in plasma was also tested. As shown in Fig. 2B, after incubation with plasma for 8 h, RDP3 was completely degraded, with a half-life of 1.7 h (calculated using GraphPad Prism software).

FITC-RDP3 was synthesized to observe peptide distribution in mice after injection. As shown in Fig. 2C, after intraperitoneal injection, the peptide was rapidly distributed to the whole intraperitoneal area. Front and back images of the mice were obtained by *in vivo* fluorescence imaging. Results showed that 60 min after injection, the peptide was mainly distributed in the abdominal cavity of mice, especially the liver and kidney.

The novel anti-hyperuricemic peptide RDP1 (AAAAGAKAR), identified in previous study, shows complete degradation in plasma at 20 min, with a half-life of 4.6 min[11]. In this research, RDP3 showed increased plasma stability (half-life: 1.7 h), which may be due its post-translation modification (-NH2). Stability testing under other conditions also confirmed better stability of RDP3 compared with RDP1. Thus, RDP3 showed characteristics of long-term maintenance at 4 °C and 37 °C and short-

term maintenance at 60 °C, which is a good advantage for its transportation and preservation. Moreover, its excellent stability in plasma also suggests good long-term maintenance *in vivo*.

RDP3 Significantly Decreased Serum Uric Acid & Alleviated Renal Damage

As the biochemical basis of gout, uncontrolled HUA can lead to the accumulation of uric acid crystals in the kidney as well as serious renal damage[28, 29]. To understand the anti-HUA and nephrotic activity of RDP3, a HUA mouse model was established by POX and adenine treatment to simulate the pathological characteristics of HUA (e.g., increase in serum uric acid level and renal damage)[5]. As shown in Fig. 3A, serum uric acid levels were significantly higher in the model group (65.0 ± 5.2 mg/L) than in the control group (23.4 ± 1.8 mg/L) ($P < 0.001$), indicating the successful establishment of HUA in mice. Serum uric acid levels were significantly lower in the Allo and Benz groups than in the HUA mice ($P < 0.001$). Serum uric acid concentrations in the RDP3 groups (100 μg/kg, 500 μg/kg, and 1 mg/kg) were 54.0 ± 0.7 mg/L, 44.2 ± 0.3 mg/L, and 39.5 ± 0.4 mg/L, respectively ($P < 0.001$ vs. Model). These results show that RDP3 had the ability to reduce serum uric acid levels, with the effects found to be concentration dependent. Moreover, RDP3 (1 mg/kg) showed similar effects as the positive control, but at a much lower dosage.

As shown in Fig. 3B, the serum creatinine level in the model group was about seven times higher than that in the control group ($P < 0.001$ vs. Control on day 7), whereas the serum creatinine levels in the Allo (12 mg/kg) and Benz groups (8

mg/kg) were significantly lower ($P < 0.001$ vs. Model on day 7). The serum creatinine levels in the RDP3 groups (100 μg/kg, 500 μg/kg, and 1 mg/kg) were 103.5 ± 36.9 μM, 65.3 ± 24.2 μM, and 36.5 ± 3.2 μM, respectively. Thus, RDP3 reduced serum creatinine levels in a concentration dependent manner. In addition, RDP3 at 1 mg/kg showed stronger activity than that of Allo and Benz. Furthermore, RDP3 at 500 μg/kg and 100 μg/kg showed stronger renal function improvement ability than Benz at 8 mg/kg.

H&E staining was performed to evaluate the ability of RDP3 to alleviate renal injury at the tissue level. As shown in Fig. 3C, the renal tubule borders in the control group were clear and epithelial cells showed ordered arrangement. In contrast, the kidneys of HUA mice showed indistinct boundaries between adjacent proximal convoluted tubules, as well as tubular atrophy. These findings are consistent with the serum creatinine results, with RDP3 and positive control treatment relieving the renal pathological changes observed in HUA mice.

In HUA animals, RDP1 and RDP3 reduced uric acid levels by 49.7% ± 2.2% and 39.2% ± 0.6%, respectively, suggesting that RDP3 had a weaker ability at reducing uric acid than RDP1 (1 mg/kg) (100% for model group). In contrast, RDP3 decreased creatinine levels by almost twice that of RDP1, i.e., 86.0% ± 1.1% and 41.3% ± 8.8%, respectively (100% for model group). Both Allo and Benz are considered first-line drugs for the rapid clinical treatment of excess uric acid[8]. Here, at a low concentration of 1 mg/kg, RDP3 showed a similar reduction in uric acid as produced by the positive control, but with far better renal protective ability than either Allo or

Benz (12 mg/kg and 8 mg/kg). In addition, given its safe extraction from edible rice, the risk of adverse reactions to RDP3 is low. Thus, RDP3 exhibits great potential as a drug candidate against HUA, especially in the treatment of HUA-related nephropathy.

RDP3 Inhibited XOD Activity & URAT1 Expression in Mice

Uric acid is the final product of purine metabolism[30]. Under normal physiological conditions, purine is metabolized in the liver via enzymatic action, e.g., XOD, with the resulting uric acid predominantly excreted via the kidney in urine[31]. Renal transporters in proximal convoluted tubules, e.g., URAT1, play important roles in this process[32]. To elucidate the mechanism related to the reduction of uric acid by RDP3, molecular docking of RDP3 with XOD and URAT1 was performed. As shown in Fig. S2A-D, RDP3 was combined in the larger cavity of XOD with a curl conformation. The combination of RDP3 and URAT1, as is shown in Fig. S2E-H, results demonstrated that RDP3 combined with the hydrophobic core surrounded by the spiral structure of URAT1, which formed three hydrogen bonds. The affinities of RDP3 with XOD and URAT1 were -8.0 kcal/mol and -8.6 kcal/mol, respectively (lower affinity indicates better binding).

Both XOD activity and URAT1 content were detected in HUA mice. As shown in Fig. 4A, the XOD activity levels in the control, model, and Allo groups were 28.5 ± 0.5 U/L, 32.1 ± 0.4 U/L, and 19.8 ± 0.5 U/L, respectively ($P < 0.001$, Control vs. Model; $P < 0.001$ Allo vs. Model). The XOD activity levels in the RDP3 groups (100 μg/kg, 500 μg/kg, and 1 mg/kg) were 28.6 ± 0.4 U/L, 27.8 ± 1.0 U/L, and 23.4 ± 1.4

U/L, respectively. These results suggest that RDP3 treatment effectively reduced XOD activity in HUA mice in a concentration dependent manner, as confirmed by XOD activity in the liver of HUA mice (Fig. 4B).

The direct interaction of RDP3 with XOD *in vitro* was also detected. As shown in Fig. S3, RDP3 inhibited XOD concentration dependently. Notably, the XOD inhibitory ability of RDP3 (1 mg/kg) *in vivo* was similar to that of Allo (10 mg/kg), whereas the XOD inhibitory rate *in vitro* (RDP3, 1 mg/mL, 29.45%±11.15%) was only a quarter of that of Allo (10 mg/mL, 99.97%±0.44%). As reported in previous research, short peptides can be easily degraded into smaller peptide sequences *in vivo*[12]. Therefore, it is possible that RDP3 was degraded into shorter peptide sequences *in vivo*, and its ability to inhibit XOD was enhanced accordingly.

Based on western blotting, the expression of URAT1 in the kidney of HUA mice was also detected. As shown in Fig. 4C, compared with the control group, the expression of URAT1 in the model group increased significantly, whereas under RDP3 intervention (500 μg/kg and 1 mg/kg), the expression of URAT1 in the kidney of HUA mice decreased significantly, suggesting that RDP3 reduced uric acid by inhibiting the expression of URAT1. These results also suggest that RDP3 may target XOD and URAT1 at the same time to reduce uric acid in HUA mice.

It is worth noting that the HUA mouse model was constructed using POX and adenine. POX was used to inhibit uricase and thus increase the level of uric acid *in vivo*, whereas adenine was used to increase purine intake and simulate HUA nephropathy[11]. Therefore, when preparing HUA mice, it is necessary to consider the

activity of the active peptide. It is possible that the sample may decrease uric acid by antagonizing POX and or enhancing uricase. In this research, the novel peptide not only inhibited XOD activity, but also reduced URAT1 expression. Therefore, it could be concluded that part of the role of RDP3 in reducing uric acid comes from its influence on the production and excretion of uric acid. In addition, at present, there is no approved anti-hyperuricemic medicine that can both inhibit XOD activity and decrease the expression of URAT1. Even for published anti-hyperuricemic peptides, a similar ability to decrease uric acid through multiple targets, as found for RDP3, has not been reported[11-13, 18-20]. Thus, these results suggest that RDP3 has great potential in the development of new drugs for the treatment of gout.

RDP3 Reduced Inflammation in Kidneys of HUA Mice

The accumulation of uric acid in the kidney can cause repeated inflammation and subsequent renal injury[33]. Inflammation plays an important role in the development of HUA nephropathy, which is a common and serious complication of gout[34]. In HUA, excessive accumulation of uric acid stimulates the action of the NLR family, including the pyrin domain inflammatory complex (composed of NLRP3, ASC, and pro-caspase-1). The assembled NLRP3 inflammasome can cause secretion of mature IL-1β, which is the main cause of renal injury in HUA[35-37].

As shown in Fig. 4D, the level of IL-1β in the model group increased significantly compared with that in the control group, indicating that HUA led to an increase in the inflammatory response of mice. Both Allo (10 mg/kg) and RDP3 treatment (100 μg/kg, 500 μg/kg, and 1 mg/kg) successfully reduced this inflammatory response,

418 with RDP3 (500 μg/kg and 1 mg/kg) exhibiting better anti-inflammatory ability than
419 Allo.

420 Western blot analysis was used to detect NLRP3 inflammasome expression
421 (NLRP3, ASC, and caspase-1) in the kidneys of mice. As shown in Fig. 4E-H, the
422 NLRP3, ASC, and caspase-1 contents in the kidneys of the model group were
423 significantly higher than those of the Allo group, suggesting that the NLRP3
424 inflammasome was activated. In the RDP3 groups (500 μg/kg and 1 mg/kg), NLRP3
425 inflammasome expression (NLRP3, ASC, and caspase-1) decreased significantly.
426 These results show that RDP3 may reduce inflammation by inhibiting NLRP3
427 inflammasome expression to alleviate renal damage.

428 **RDP3 Showed Analgesic & Anti-inflammatory Activity**

429 Long-term HUA will increase the crystallization risk of urate in circulation, which
430 may be deposited in joints, causing severe pain, joint deformity, and reduced quality
431 of life[1, 38]. Gout is a disease caused by the secretion of inflammatory cytokines, such
432 as IL-1β and TNF-α, which is a key point in gout treatment[38]. In view of the excellent
433 anti-inflammatory ability of RDP3 in HUA nephropathy, RDP3 may play a therapeutic
434 role in acute gout attack.

435 The effect of RDP3 on inflammatory pain was detected. As seen in Fig. S4,
436 RDP3 showed significant and concentration-dependent pain relief. Of note, the
437 analgesic effect of RDP3 at 1 mg/kg was stronger than that of DS at 12 mg/kg. As
438 shown in Fig. 5A, the paw swelling rate in mice peaked on the first day after
439 injection. The swelling rates of the model and DS groups (12 mg/kg) were 50.6% ±

7.1% and 32.5% ± 7.5%, respectively, suggesting that the DS group (12 mg/kg) showed significant alleviative effects on swelling caused by MSU ($P < 0.001$). The swelling rates of the RDP3 groups (100 μg/kg, 500 μg/kg, and 1 mg/kg) were 30.6% ± 8.1%, 29.6% ± 7.9%, and 24.4% ± 6.5%, respectively. Thus, all RDP3 groups showed stronger anti-inflammatory swelling ability than that of DS at lower concentrations.

To verify the effect of RDP3 on inflammatory swelling induced by MSU, the levels of TNF-α and IL-1β in mouse feet were detected. As shown in Fig. 5B and C, compared with the saline group, the RDP3 (500 μg/kg and 1 mg/kg) and DS groups (12 mg/kg) significantly reduced the level of TNF-α; the RDP3 (100 μg/kg, 500 μg/kg, and 1 mg/kg) and DS groups (12 mg/kg) also significantly reduced the level of IL-1β ($P < 0.001$ vs. Saline). It is worth noting that the anti-inflammatory activity of RDP3 at 1 mg/kg was better than that of DS at 12 mg/kg. H&E staining of feet also confirmed the positive effect of RDP3 on MSU injury recovery. As shown in Fig. 5D, loose connective tissue edema in the model group was thickened and inflammatory cells were increased, which were significantly reduced in the RDP3 and DS groups. These results show that RDP3 not only had a significant anti-HUA ability, but also showed excellent anti-inflammatory and analgesic capabilities.

A multi-functional anti-HUA peptide (RDP3) was identified in the current research, which not only inhibited XOD activity but also decreased URAT1 expression. RDP3 also reduced renal damage in HUA mice by decreasing NLRP3 inflammasome expression and, at the same time, showed excellent anti-

462 inflammatory and analgesic abilities. RDP3 not only provides a drug candidate for
463 the research and development of anti-gout medicines, but also suggests the
464 potential that Yunnan-derived *O. sativa* may be a healthy and nutritious food for
465 patients with HUA and gout, which is expected to promote the development of the
466 local planting industry.

467 **Author Information**

468 *Corresponding Author

469 Dr. Xinwang Yang: yangxinwanghp@163.com

470 Dr. Jun Sun: sunjun6661@126.com

471 **Author Contributions**

472 †Naixin Liu and Ying Wang contributed equally to this work.

473 **Notes**

474 The authors declare no competing financial interests.

475 **Acknowledgements**

476 This work was supported by grants from the Yunnan Applied Basic Research Project
477 Foundation (2019FB128 and 2017FB035), National Natural Science Foundation of
478 China (81760648, 31460571, and 31670776), and Yunnan Applied Basic Research
479 Project-Kunming Medical University Union Foundation (2018FE001(−161) and
480 2019FE001(-020))

481 **Supporting Information**

482 Fig. S1, Purification of RDP3 from *O. sativa* collected from Yunnan, China; Fig. S2,
483 Molecular docking of RDP3-XOD/URAT1; Fig. S3, XOD Inhibition activity of RDP3 *in*

vitro; Fig. S4, RDP3 alleviated formalin-induced paw licking; Table S1, Hemolytic activity of RDP3; Table 2, Acute toxicity of RDP3.

References

1. Chilappa, C. S.; Aronow, W. S.; Shapiro, D.; Sperber, K.; Patel, U.; Ash, J. Y., Gout and hyperuricemia. *Compr Ther* **2010**, *36*, 3-13.

2. Kim, S. C.; Di Carli, M. F.; Garg, R. K.; Vanni, K.; Wang, P.; Wohlfahrt, A.; Yu, Z.; Lu, F.; Campos, A.; Bibbo, C. F.; Smith, S.; Solomon, D. H., Asymptomatic hyperuricemia and coronary flow reserve in patients with metabolic syndrome. *BMC Rheumatol* **2018**; *2:* 17.

3. Kuo, D.; Crowson, C. S.; Gabriel, S. E.; Matteson, E. L., Hyperuricemia and incident cardiovascular disease and noncardiac vascular events in patients with rheumatoid arthritis. *Int J Rheumatol* **2014**, *2014*, 523897.

4. Burns, C. M.; Wortmann, R. L., Gout therapeutics: new drugs for an old disease. *Lancet* **2011**, *377*, 165-77.

5. Li, X.; Yan, Z.; Carlstrom, M.; Tian, J.; Zhang, X.; Zhang, W.; Wu, S.; Ye, F., Mangiferin Ameliorates Hyperuricemic Nephropathy Which Is Associated With Downregulation of AQP2 and Increased Urinary Uric Acid Excretion. *Front Pharmacol* **2020**, *11*, 49.

6. Bao, R.; Liu, M.; Wang, D.; Wen, S.; Yu, H.; Zhong, Y.; Li, Z.; Zhang, Y.; Wang, T., Effect of Eurycoma longifolia Stem Extract on Uric Acid Excretion in Hyperuricemia Mice. *Front Pharmacol* **2019**, *10*, 1464.

7. Machado-Vieira, R.; Lara, D. R.; Souza, D. O.; Kapczinski, F., Therapeutic efficacy of allopurinol in mania associated with hyperuricemia. *J Clin Psychopharmacol* **2001**, *21*, 621-2.

8. Zhou, Q.; Su, J.; Zhou, T.; Tian, J.; Chen, X.; Zhu, J., A study comparing the safety and

efficacy of febuxostat, allopurinol, and benzbromarone in Chinese gout patients: a retrospective cohort study. *Int J Clin Pharmacol Ther* **2017**, *55*, 163-168.

9. Martens, K. L.; Khalighi, P. R.; Li, S.; White, A. A.; Silgard, E.; Frieze, D.; Estey, E.; Garcia, D. A.; Hingorani, S.; Li, A., Comparative effectiveness of rasburicase versus allopurinol for cancer patients with renal dysfunction and hyperuricemia. *Leuk Res* **2020**, *89*, 106298.

10. Bensman, A., Non-steroidal Anti-inflammatory Drugs (NSAIDs) Systemic Use: The Risk of Renal Failure. *Front Pediatr* **2019**, *7*, 517.

11. Liu, N.; Wang, Y.; Yang, M.; Bian, W.; Zeng, L.; Yin, S.; Xiong, Z.; Hu, Y.; Wang, S.; Meng, B.; Sun, J.; Yang, X., New Rice-Derived Short Peptide Potently Alleviated Hyperuricemia Induced by Potassium Oxonate in Rats. *J Agric Food Chem* **2019**, *67*, 220-228.

12. Murota, I.; Taguchi, S.; Sato, N.; Park, E. Y.; Nakamura, Y.; Sato, K., Identification of antihyperuricemic peptides in the proteolytic digest of shark cartilage water extract using in vivo activity-guided fractionation. *J Agric Food Chem* **2014**, *62*, 2392-7.

13. Li, Q.; Kang, X.; Shi, C.; Li, Y.; Majumder, K.; Ning, Z.; Ren, J., Moderation of hyperuricemia in rats via consuming walnut protein hydrolysate diet and identification of new antihyperuricemic peptides. *Food Funct* **2018**, *9*, 107-116.

14. Malhan, S.; Guler, S.; Yetkin, I.; Baeten, S.; Verheggen, B., Cost-Effectiveness of Exenatide Twice Daily (Bid) Added To Basal Insulin Compared To A Bolus Insulin Add-On In Turkey. *Value Health* **2014**, *17*, A349.

15. Higuchi, S.; Murayama, N.; Saguchi, K.; Ohi, H.; Fujita, Y.; da Silva, N. J., Jr.; de Siqueira, R. J.; Lahlou, S.; Aird, S. D., A novel peptide from the ACEI/BPP-CNP precursor in the venom

528 of Crotalus durissus collilineatus. *Comp Biochem Physiol C Toxicol Pharmacol* **2006**, *144*,
529 107-21.
530 16. Wang, Y.; Li, X.; Yang, M.; Wu, C.; Zou, Z.; Tang, J.; Yang, X., Centipede venom peptide
531 SsmTX-I with two intramolecular disulfide bonds shows analgesic activities in animal models.
532 *J Pept Sci* **2017**, *23*, 384-391.
533 17. Yang, X.; Lee, W. H.; Zhang, Y., Extremely abundant antimicrobial peptides existed in
534 the skins of nine kinds of Chinese odorous frogs. *J Proteome Res* **2012**, *11*, 306-19.
535 18. Nongonierma, A. B.; Fitzgerald, R. J., Tryptophan-containing milk protein-derived
536 dipeptides inhibit xanthine oxidase. *Peptides* **2012**, *37*, 263-72.
537 19. He, W.; Su, G.; Sun-Waterhouse, D.; Waterhouse, G. I. N.; Zhao, M.; Liu, Y., In vivo anti-
538 hyperuricemic and xanthine oxidase inhibitory properties of tuna protein hydrolysates and its
539 isolated fractions. *Food Chem* **2019**, *272*, 453-461.
540 20. Li, Y.; Kang, X.; Li, Q.; Shi, C.; Lian, Y.; Yuan, E.; Zhou, M.; Ren, J., Anti-hyperuricemic
541 peptides derived from bonito hydrolysates based on in vivo hyperuricemic model and in vitro
542 xanthine oxidase inhibitory activity. *Peptides* **2018**, *107*, 45-53.
543 21. Bian, W.; Meng, B.; Li, X.; Wang, S.; Cao, X.; Liu, N.; Yang, M.; Tang, J.; Wang, Y.;
544 Yang, X., OA-GL21, a novel bioactive peptide from Odorrana andersonii, accelerated the
545 healing of skin wounds. *Biosci Rep* **2018**, *38*.
546 22. Liu, N.; Li, Z.; Meng, B.; Bian, W.; Li, X.; Wang, S.; Cao, X.; Song, Y.; Yang, M.; Wang,
547 Y.; Tang, J.; Yang, X., Accelerated Wound Healing Induced by a Novel Amphibian Peptide
548 (OA-FF10). *Protein Pept Lett* **2019**, *26*, 261-270.
549 23. Haryono, A.; Nugrahaningsih, D. A. A.; Sari, D. C. R.; Romi, M. M.; Arfian, N., Reduction

550 of Serum Uric Acid Associated with Attenuation of Renal Injury, Inflammation and
551 Macrophages M1/M2 Ratio in Hyperuricemic Mice Model. *Kobe J Med Sci* **2018**, *64*, E107-
552 E114.
553 24. Trott, O.; Olson, A. J., AutoDock Vina: improving the speed and accuracy of docking with
554 a new scoring function, efficient optimization, and multithreading. *J Comput Chem* **2010**, *31*,
555 455-61.
556 25. Chen, Y.; Li, C.; Duan, S.; Yuan, X.; Liang, J.; Hou, S., Curcumin attenuates potassium
557 oxonate-induced hyperuricemia and kidney inflammation in mice. *Biomed Pharmacother* **2019**,
558 *118*, 109195.
559 26. Li, C.; Chen, M.; Li, X.; Yang, M.; Wang, Y.; Yang, X., Purification and function of two
560 analgesic and anti-inflammatory peptides from coelomic fluid of the earthworm, Eisenia
561 foetida. *Peptides* **2017**, *89*, 71-81.
562 27. Parashar, P.; Mazhar, I.; Kanoujia, J.; Yadav, A.; Kumar, P.; Saraf, S. A.; Saha, S.,
563 Appraisal of anti-gout potential of colchicine-loaded chitosan nanoparticle gel in uric acid-
564 induced gout animal model. *Arch Physiol Biochem* **2019**, 1-11.
565 28. Han, J.; Wang, X.; Tang, S.; Lu, C.; Wan, H.; Zhou, J.; Li, Y.; Ming, T.; Wang, Z. J.; Su,
566 X., Protective effects of tuna meat oligopeptides (TMOP) supplementation on hyperuricemia
567 and associated renal inflammation mediated by gut microbiota. *FASEB J* **2020**, *34*, 5061-5076.
568 29. Cui, D.; Liu, S.; Tang, M.; Lu, Y.; Zhao, M.; Mao, R.; Wang, C.; Yuan, Y.; Li, L.; Chen,
569 Y.; Cheng, J.; Lu, Y.; Liu, J., Phloretin ameliorates hyperuricemia-induced chronic renal
570 dysfunction through inhibiting NLRP3 inflammasome and uric acid reabsorption.
571 *Phytomedicine* **2020**, *66*, 153111.

572 30. Yamada, Y., [Hyperuricemia associated with inborn errors of purine metabolism:
573 screening, enzymatic and genetic diagnosis]. *Nihon Rinsho* **2003**, *61 Suppl 1*, 278-83.
574 31. Rudnicka, R.; Bojarska, E.; Kazimierczuk, Z., Benzimidazole derivatives as potent
575 inhibitors of milk xanthine oxidase. *Acta Pol Pharm* **2004**, *61 Suppl*, 37-9.
576 32. Wu, X. H.; Zhang, J.; Wang, S. Q.; Yang, V. C.; Anderson, S.; Zhang, Y. W., Riparoside
577 B and timosaponin J, two steroidal glycosides from Smilax riparia, resist to hyperuricemia
578 based on URAT1 in hyperuricemic mice. *Phytomedicine* **2014**, *21*, 1196-201.
579 33. Peng, A.; Lin, L.; Zhao, M.; Sun, B., Identifying mechanisms underlying the amelioration
580 effect of Chrysanthemum morifolium Ramat. 'Boju' extract on hyperuricemia using
581 biochemical characterization and UPLC-ESI-QTOF/MS-based metabolomics. *Food Funct*
582 **2019**, *10*, 8042-8055.
583 34. Singh, J. A., Gout: will the "King of Diseases" be the first rheumatic disease to be cured?
584 *BMC Med* **2016**, *14*, 180.
585 35. Wang, K.; Hu, L.; Chen, J. K., RIP3-deficience attenuates potassium oxonate-induced
586 hyperuricemia and kidney injury. *Biomed Pharmacother* **2018**, *101*, 617-626.
587 36. Tan, J.; Wan, L.; Chen, X.; Li, X.; Hao, X.; Li, X.; Li, J.; Ding, H., Conjugated Linoleic
588 Acid Ameliorates High Fructose-Induced Hyperuricemia and Renal Inflammation in Rats via
589 NLRP3 Inflammasome and TLR4 Signaling Pathway. *Mol Nutr Food Res* **2019**, *63*, e1801402.
590 37. Chen, L.; Lan, Z., Polydatin attenuates potassium oxonate-induced hyperuricemia and
591 kidney inflammation by inhibiting NF-kappaB/NLRP3 inflammasome activation via the
592 AMPK/SIRT1 pathway. *Food Funct* **2017**, *8*, 1785-1792.
593 38. Di Fiore, I. J.; Holloway, G.; Coulson, B. S., Innate immune responses to rotavirus

infection in macrophages depend on MAVS but involve neither the NLRP3 inflammasome nor JNK and p38 signaling pathways. *Virus Res* **2015**, *208*, 89-97.

Figure Captions

Figure 1. Structure of RDP3.

A. Molecular weight of RDP3 (785.97 Da).

B. Primary structure of RDP3 (AAAAMAGPK-NH2).

Figure 2. Characteristics of RDP3.

A. RDP3 showed great stability under 4 °C, 37 °C, and 60 °C and during repeated freezing and thawing (n = 3).

B. Half-life of RDP3 incubated with plasma was 1.7 h, with complete degradation within 8 h (n = 3).

C. Images after injection of FITC-RDP3.

Figure 3. RDP3 Reduced Uric Acid Level and Alleviated Kidney Damage in Hyperuricemic Mice.

A. RDP3 induced a concentration-dependent decrease in serum uric acid in hyperuricemic mice (n = 6).

B. RDP3 significantly reduced serum creatinine levels in mice (n = 6).

C. Control group showed orderly arranged epithelial cells. Model group showed disappearance of brush border and tubular atrophy, with RDP3 and Allo treatment relieving renal injury.

###/****P* < 0.001 indicates significantly different from control (Student's *t*-tests).

Figure 4. RDP3 Decreased XOD Activity and Showed Anti-inflammatory

Activity in Mice.

RDP3 decreased XOD activity in serum (A) and liver (B) in a concentration-dependent manner (n = 6), and decreased expression of URAT1 in kidneys (C, n = 3). RDP3 (100 μg/kg, 500 μg/kg, and 1 mg/kg) decreased serum levels of IL-1β in mice in a concentration-dependent manner. NLRP3 inflammasome expression levels in hyperuricemic mice were detected by western blot analysis, followed by quantitative analysis (E) (n = 3). F-H show quantitative analysis results, in which RDP3 reduced NLRP3 inflammasome expression (NLRP3, ASC, and caspase-1). $^{\#}/^{*}P < 0.05$, $^{\#\#}/^{**}P < 0.01$, and $^{\#\#\#}/^{***}P < 0.001$ indicate significantly different from control (Student's *t*-tests).

Figure 5. RDP3 Reduced Foot Swelling in Mice Injected with MSU and Decreased Inflammation in Mice.

A. RDP3 showed concentration-dependent reduction in paw swelling induced by MSU (n = 6).

B. RDP3 (100 μg/kg, 500 μg/kg, and 1 mg/kg) induced a concentration-dependent decrease in IL-1β level in paw tissue of mice (n = 6).

C. RDP3 (100 μg/kg and 500 μg/kg) reduced serum level of TNF-α in mice (n = 6).

D. RDP3 alleviated tissue injury caused by MSU injection.

$^{\#\#\#}/^{***}P < 0.001$ indicates significantly different from control (Student's *t*-tests).

Figures

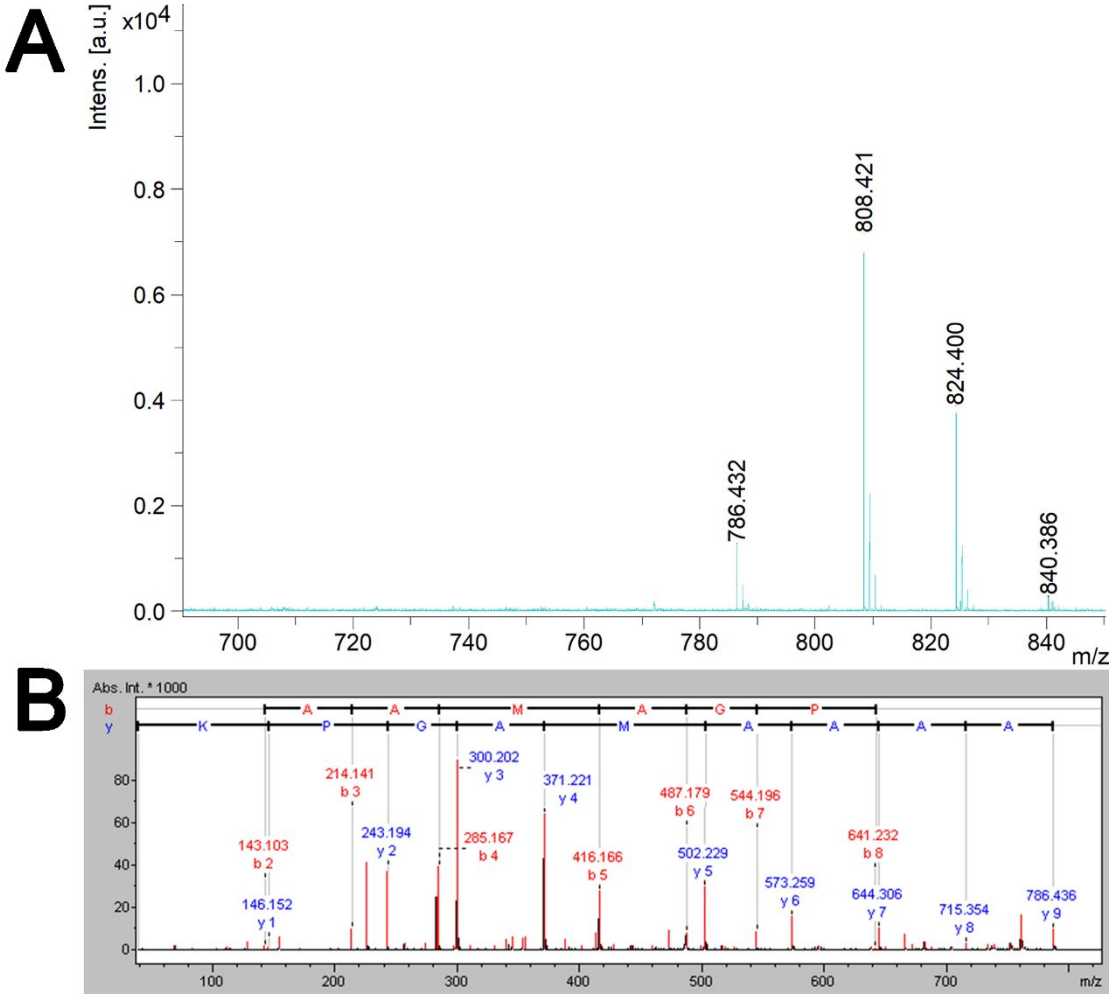

Figure 1

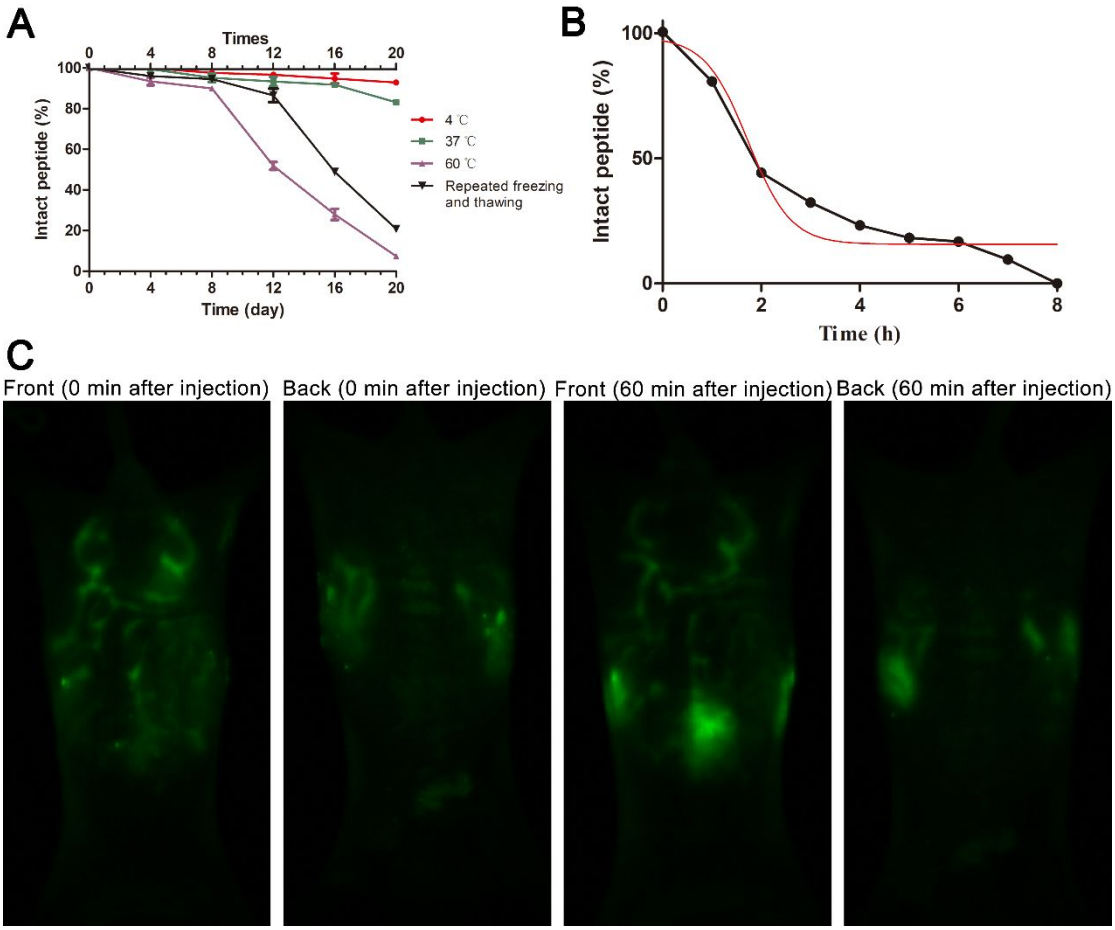
A
Times
Intact peptide (%)
Time (day)
4 ℃
37 ℃
60 ℃
Repeated freezing and thawing
B
Intact peptide (%)
Time (h)
C
Front (0 min after injection)
Back (0 min after injection)
Front (60 min after injection)
Back (60 min after injection)

Figure 2

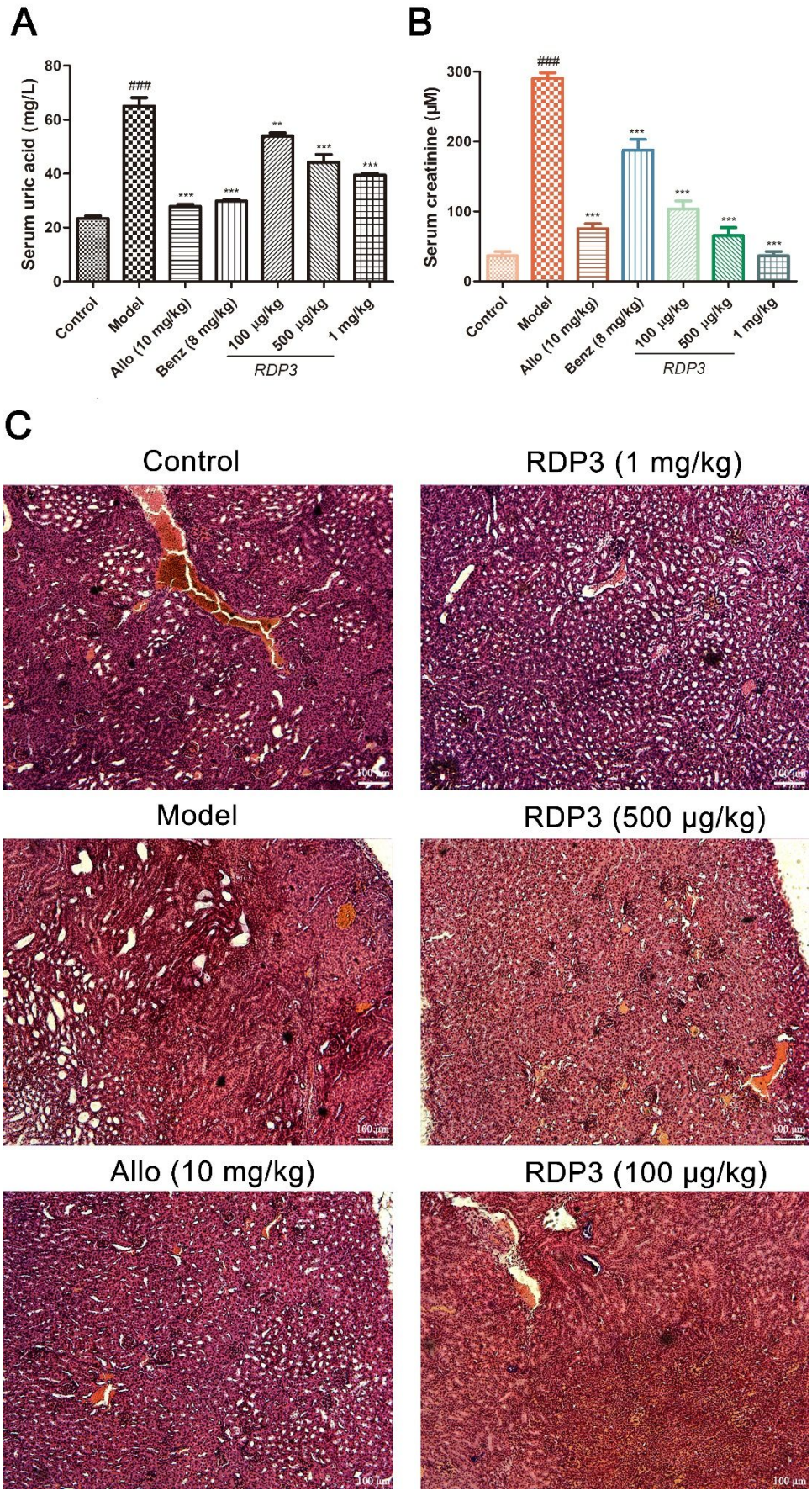
A
Serum uric acid (mg/L)
0
20
40
60
80
###
**
***
Control
Model
Allo (10 mg/kg)
Benz (8 mg/kg)
100 μg/kg
500 μg/kg
1 mg/kg
RDP3
B
Serum creatinine (μM)
0
100
200
300
###
***
Control
Model
Allo (10 mg/kg)
Benz (8 mg/kg)
100 μg/kg
500 μg/kg
1 mg/kg
RDP3
C
Control
RDP3 (1 mg/kg)
Model
RDP3 (500 μg/kg)
Allo (10 mg/kg)
RDP3 (100 μg/kg)
100 μm

Figure 3

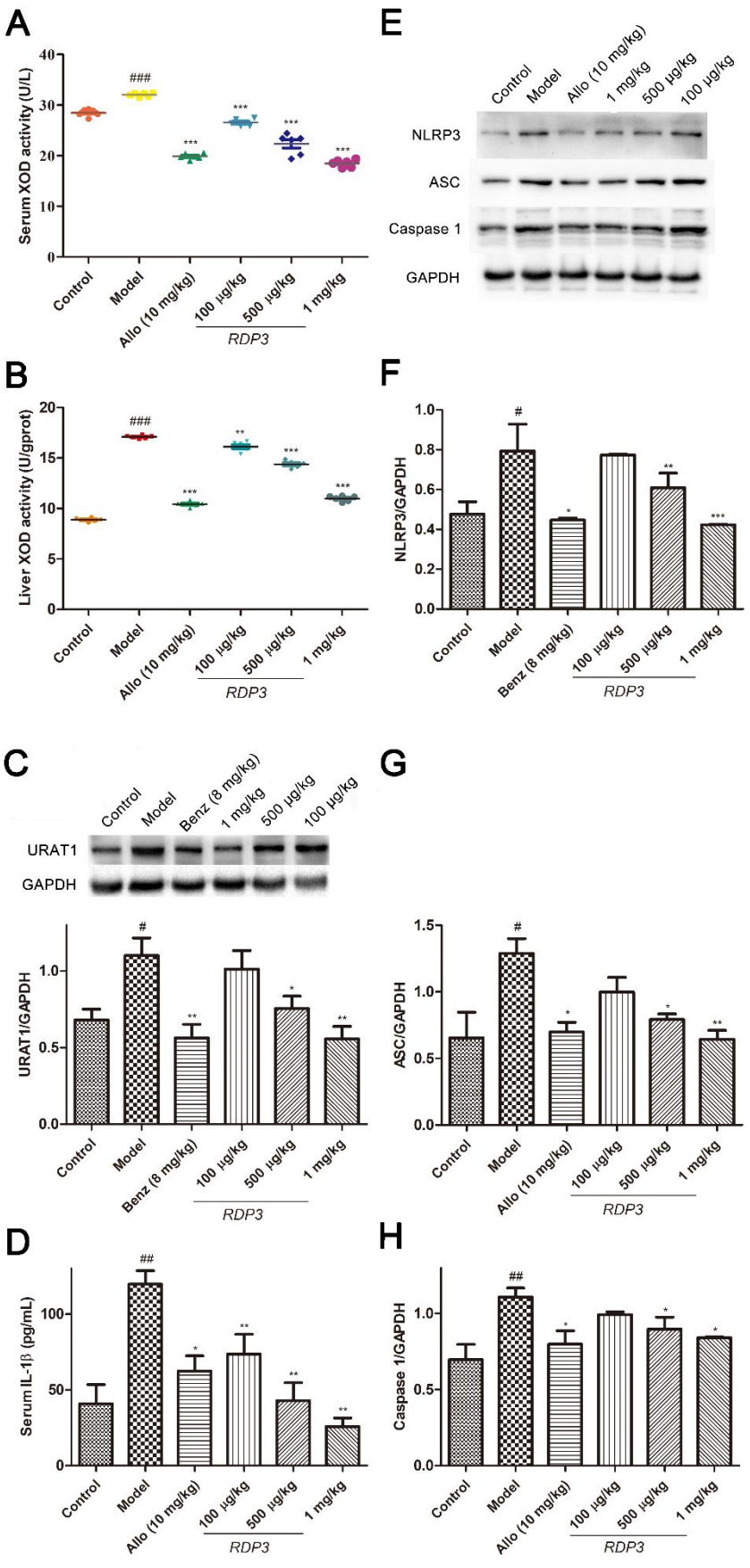
A
Serum XOD activity (U/L)
###
***
Control
Model
Allo (10 mg/kg)
100 μg/kg
500 μg/kg
1 mg/kg
RDP3
B
Liver XOD activity (U/gprot)
###
**
***
Control
Model
Allo (10 mg/kg)
100 μg/kg
500 μg/kg
1 mg/kg
RDP3
C
Control
Model
Benz (8 mg/kg)
1 mg/kg
500 μg/kg
100 μg/kg
URAT1
GAPDH
URAT1/GAPDH
#
**
*
Control
Model
Benz (8 mg/kg)
100 μg/kg
500 μg/kg
1 mg/kg
RDP3
D
Serum IL-1β (pg/mL)
##
*
**
Control
Model
Allo (10 mg/kg)
100 μg/kg
500 μg/kg
1 mg/kg
RDP3
E
Control
Model
Allo (10 mg/kg)
1 mg/kg
500 μg/kg
100 μg/kg
NLRP3
ASC
Caspase 1
GAPDH
F
NLRP3/GAPDH
#
*
**
***
Control
Model
Benz (8 mg/kg)
100 μg/kg
500 μg/kg
1 mg/kg
RDP3
G
ASC/GAPDH
#
*
**
Control
Model
Allo (10 mg/kg)
100 μg/kg
500 μg/kg
1 mg/kg
RDP3
H
Caspase 1/GAPDH
##
*
Control
Model
Allo (10 mg/kg)
100 μg/kg
500 μg/kg
1 mg/kg
RDP3

Figure 4

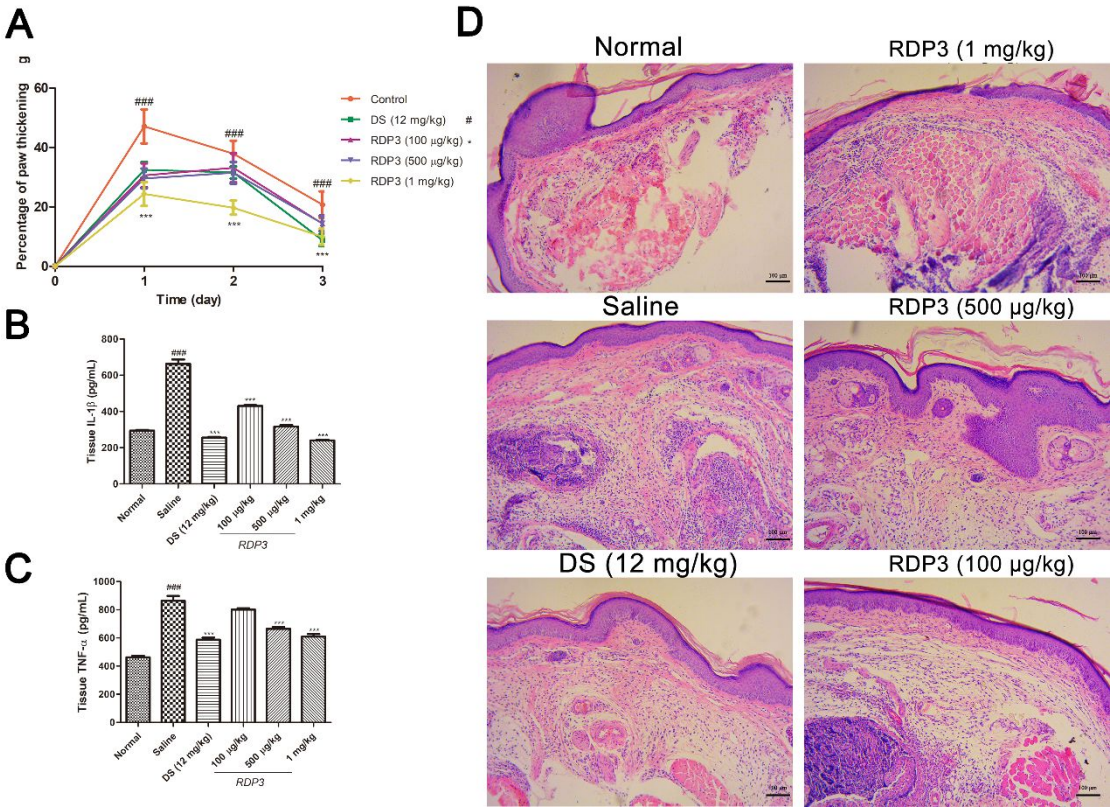
A
g
Percentage of paw thickening
Time (day)
Control
DS (12 mg/kg)
RDP3 (100 μg/kg)
RDP3 (500 μg/kg)
RDP3 (1 mg/kg)
B
Tissue IL-1β (pg/mL)
C
Tissue TNF-α (pg/mL)
Normal
Saline
DS (12 mg/kg)
100 μg/kg
500 μg/kg
1 mg/kg
RDP3
D
Normal
RDP3 (1 mg/kg)
Saline
RDP3 (500 μg/kg)
DS (12 mg/kg)
RDP3 (100 μg/kg)

Figure 5

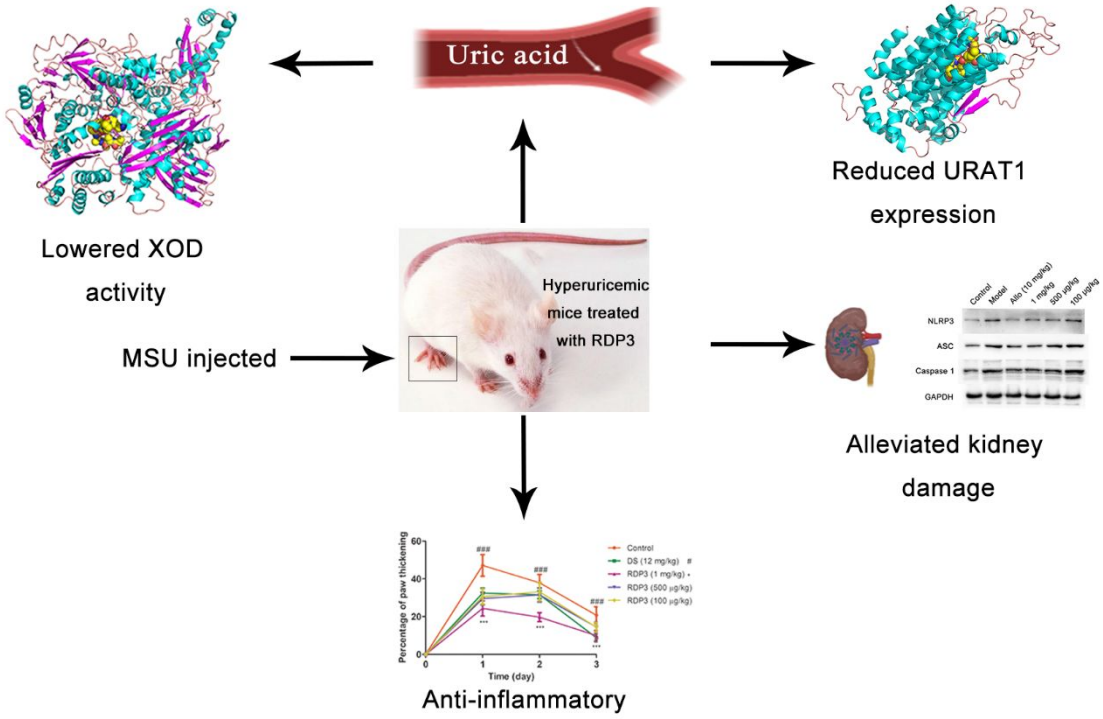

Table of Contents Graphic